OXYGEN, CA, AND TI ISOTOPIC COMPOSITIONS OF HIBONITE-BEARING INCLUSIONS. T. Ushikubo, H. Hiyagon, and N. Sugiura, Department of Earth and Planetary Science, University of Tokyo, 7-3-1 Hongo, Bunkyo, Tokyo, 113-0033, Japan (ushi@eps.s.u-tokyo.ac.jp).

Introduction: Mass independent isotopic anomalies of O, Ca, and Ti of refractory inclusions are evidence for existence of isotopic heterogeneity in the early solar nebula. Oxygen isotopic anomaly of $\delta^{17}O \sim \delta^{18}O \sim -50$ permil is commonly observed in refractory inclusions and is distinct from those of other chondritic materials [1]. This suggests that refractory inclusions were derived from a common ^{16}O-rich reservoir. In contrast, large isotopic anomalies of Ca and Ti (especially neutron-rich isotopes, ^{48}Ca and ^{50}Ti) are typically observed in hibonite-bearing inclusions [2-5]. This suggests that some hibonite-bearing inclusions were derived from a reservoir different from that of common refractory inclusions. However, the relationship between the ^{16}O-rich reservoir and the reservoir of Ca and Ti isotopic anomalies has not been established because O isotopic compositions of hibonite-bearing inclusions with Ca and Ti isotopic anomalies [6-8]. In the present study, O, Ca, and Ti isotopic compositions of hibonite-bearing inclusions were measured.

Samples: Eight platelet hibonites, or PLACs (Kz1-11, MC-F5, -F9, -F19, -F23, -F73, -F75, and –F76), one HAL-type hibonite inclusion (Kz1-2), one hibonite-pyroxene spherule (Kz1-9), one spinel-hibonite inclusion, or SHIB (MC-F13), and one spinel-pyroxene inclusion (MC-F58C) were found from a thin section of Kainsaz (CO3.2; labeled as Kz1-*) and fragments of freeze-thaw disaggregation of Murchison (CM2; labeled as MC-F*). For classification of hibonite-bearing inclusions, please refer to [5].

PLACs: Kz1-11, 250 μm×250 μm in size, is an aggregate of blade-shape hibonite grains. Thin spinel and diopside rim structure (<10 μm) were observed. MC-F5, 80μm×60μm in size, is probably an isolated hibonite grain because remnants of matrix are found around this inclusion. Tiny perovskite and ZrO_2 grains are enclosed in hibonite. MC-F9, 80 μm×60 μm in size, and MC-F23, 90 μm×80 μm in size, are fragments of a much larger hibonite grain. Spinel was observed between hibonite and remnants of matrix, which suggest that these inclusions originally consist of a hibonite grain and a spinel rim. MC-F19, 110 μm×40 μm in size, and MC-F73, 130 μm×50 μm in size, are fragments of a much larger hibonite grain. MC-F75, 60 μm×50 μm in size, and MC-F76, 70 μm×40 μm in size, are fragments of hibonite aggregates. In MC-F75, tiny perovskite grains were observed in the grain boundary of hibonite. TiO_2 content of hibonite of PLACs is 1.5-2.5 wt.% but that of MC-F76 is about 3.8 wt.%.

HAL-type: Kz1-2, 100 μm×100 μm in size, consists of a hibonite grain enclosed by a thin spinel rim (~5μm). Small corundum grains (< a few μm) are on the outer margin of hibonite. TiO_2 content of hibonite is extremely low (< 0.1 wt.%). This inclusion has positively fractionated O, Ca, and Ti isotopes and ^{26}Mg-excess corresponding to the initial $^{26}Al/^{27}Al$ ratio of the canonical value [9].

Hib-Px spherule: Kz1-9, 60μm in diameter, is a spherule which consists of fassaite and small hibonite grains which are enclosed by fassaite and these are surrounded by a thin diopside rim (<5 μm) . Al_2O_3 content of fassaite is 25.5-35.0 wt.% and TiO_2 content of hibonite is 1.4-2.0 wt.%.

SHIB: MC-F13, 90 μm×60 μm in size, is a fragment of a much larger inclusion which consists of hibonite, spinel and perovskite. TiO_2 content of hibonite is about 7.8 wt.%.

Sp-Px inclusion: MC-F58C, 110 μm×80 μm in size, is a spheroidal inclusion and consists of spinel and perovskite with many vacansies. This inclusion is surrounded by a diopside rim.

Measurements: Isotopic compositions of the samples were measured with a CAMECA ims-6f ion microprobe of the University of Tokyo. Oxygen isotopes were measured using a 19.5 kV Cs^+ ion beam of 10 to 15 μm in diameter with an intensity of 0.1 to 0.2nA. Negative secondary ions were accelerated at –9.5 kV. A mass resolving power was set to about 5,000 which is enough to resolve $^{17}O^-$ and $^{16}OH^-$ signals. All the observed data of the samples were normalized to the average of the San Carlos olivine data. Calcium and Ti isotopes were measured using a 22.5 kV O^- ion beam of 20 to 30 μm in diameter with an intensity of 0.5 to 3.0nA. Positive secondary ions were accerelated at –10.0 kV. A mass resolving power was set to about 11,000 which is enough to resolve signals of hydrides and $^{48}Ti^+$ from $^{48}Ca^+$ but not enough to resolve $^{50}V^+$ and $^{50}Cr^+$ from $^{50}Ti^+$. These signals were corrected using $^{51}V^+$ and $^{52}Cr^+$ signals assuming that the $^{50}V/^{51}V$ ratio and the $^{50}Cr/^{52}Cr$ ratio of the samples are equal to the terrestrial values. The mass dependent isotopic fractionation was corrected according to the exponential law [10].

Results: Figure 1 shows mass-independent isotopic anomalies of Ti and Ca, $\delta^{50}Ti$ and $\delta^{48}Ca$ of the

samples. Significant isotopic anomalies of ^{48}Ca and ^{50}Ti were observed in seven samples. PLACs and Hibonite-pyroxene spherules tend to show large isotopic anomalies. A positive correlation between δ^{48}Ca and δ^{50}Ti were observed. These characteristics are consistent with the previous works [11-13]. Figure 2 shows O isotopic compositions of the samples. Oxygen isotopic compositions of Kz1-2 (HAL-type) are located to the right of the CCAM line and this could be explained as a result of intense evaporative loss. Oxygen isotopic compositions of other inclusions tend to fall along the CCAM line, and notable correlation was not found between O isotopes and isotopic anomalies of ^{48}Ca and ^{50}Ti.

Discussions: Besides a HAL-type hibonite inclusion, Kz1-2, O isotopic compositions of refractory inclusions, which have both positive and negative anomalies in ^{48}Ca and ^{50}Ti, fall along the CCAM line. Although inclusions which have positive δ^{48}Ca and δ^{50}Ti tend to show less anomalous O isotopic compositions, this may be a result of later isotopic disturbance. At least, an exotic O isotopic reservoir distinct from that of common refractory inclusions is not required. The present resulta are consistent with previous works [6-8]. It seems that whole refractory inclusions were derived from a common O isotopic reservoir. The most plausible isotopic reservoir is an ^{16}O-rich nebular gas [14]. Absence of significant correlation between O isotopic compositions and istopic anomalies of δ^{48}Ca and δ^{50}Ti can be explained if refractory inclusions formed in an ^{16}O-rich environment and their O isotopes were completely homogenized with those of the surrounding nebular gas,. It has been known that there is an exclusive correlation between the occurrence of ^{26}Al and isotopic anomalies of δ^{48}Ca and δ^{50}Ti. Such an exclusive correlation is evidence for existence of exotic isotopic reservoirs that were separated either spatially or temporally [15]. If O isotopic compositions of refractory inclusions were controlled by isotopic exchange with the nebular gas, rather uniform O isotopic compositions of refractory inclusions with or without isotopic anomalies of δ^{48}Ca and δ^{50}Ti suggests that the ^{16}O-rich nebular gas widely existed in the early solar nebula.

References: [1] Clayton R. N. (2003) *Space Science Reviews, 106,* 19-32. [2] Fahey A. et al. (1985) *ApJ (Lett.), 296,* L17-L20. [3] Ireland T. R. et al. (1985) *GCA, 49,* 1989-1993. [4] Zinner E. K. et al. (1986) *ApJ. (Lett.), 311,* L103-L107. [5] Ireland T. R. (1990) *GCA, 54,* 3219-3237. [6] Fahey A. et al. (1987a) *ApJ. (Lett.), 323,* L91-L95. [7] Ireland T. R. et al. (1992) *GCA, 56,* 2503-2520. [8] Sahijpal S. et al. (2000) *LPS XXXI,* Abstract #1502. [9] Ushikubo T. et al. (2000) *LPS XXXI,* Abstract #1561. [10] Fahey A. (1988) Ph.D. thesis. [11] Fahey A. et al. (1987b) *GCA, 51,* 329-350. [12] Hinton R. W. et al. (1987) *GCA, 52,* 2573-2598. [13] Clayton R. N. et al. (1988) *Phil.Trans. R. Soc. Lond., A325,* 483-501. [14] Krot A. N. et al. (2002) *Science, 295,* 1051-1054. [15] Sahijpal S. and Goswami J. N. (1998) *ApJ. (Lett.), 509,* L137-L140.

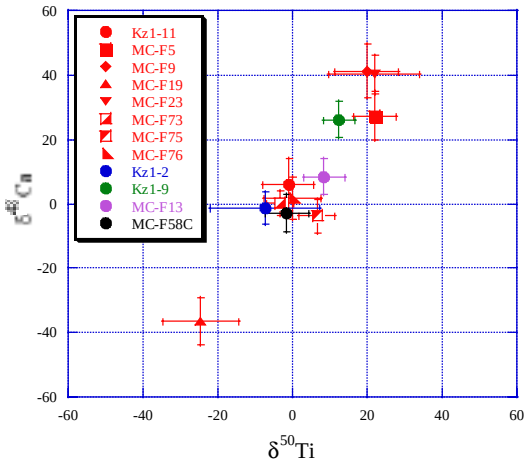

Figure 1 δ^{50}Ti and δ^{48}Ca of the present samples. Colours of symbols indicate the inclusion types: red is the PLAC, blue is the HAL-type hibonite inclusion, green is the hibonite-pyroxene spherule, purple is the SHIB, and black is the spinel-pyroxene inclusion. Errors are 2σ.

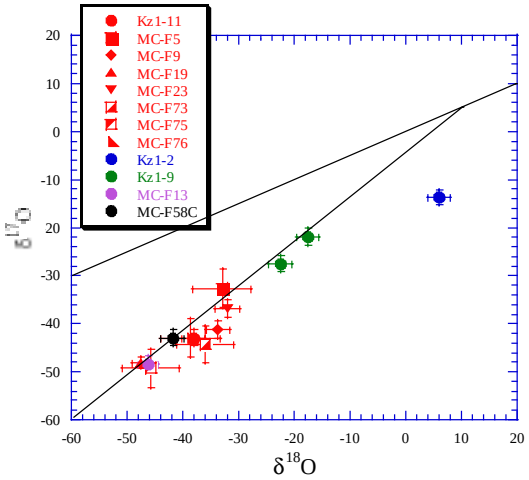

Figure 2 Oxygen isotopic compositions of the present samples. The CCAM line and the Terrestrial Fractionation line are also shown. Symbols are the same as those of Figure 1. Errors are 1σ.